Cement and Concrete Research 39 (2009) 329–339

Contents lists available at ScienceDirect

Cement and Concrete Research

journal homepage: http://ees.elsevier.com/CEMCON/default.asp

Modeling of chloride transport coupled with enhanced moisture conductivity in concrete exposed to marine environment

Prince O'Neill Iqbal [1], Tetsuya Ishida *

Concrete Laboratory, Department of Civil Engineering, The University of Tokyo Room No.334, Faculty of Engineering Bldg.1, 7-3-1 Hongo, Bunkyo-ku, Tokyo, 113-8565, Japan

ARTICLE INFO

Article history:
Received 23 March 2008
Accepted 7 January 2009

Keywords:
Chloride convection
Diffusivity
Marine environment
Sorption
Moisture conductivity

ABSTRACT

In this research, the chloride penetration in concrete is modeled under marine environment loadings. Moisture migration model is enhanced to simulate the sorption flux under submerged wetting after long exposure to drying. The non-ideal viscosity of flow in the porous media is modified according to the nature of micro-pore structure by modeling the sensitivity of different porous networks (dense and coarse) to react towards the external environment. The strong sorption flux generated as a result of wetting and drying cyclic exposure is modeled by applying hydraulic pressure at the exposed surface. Chloride profiles are then simulated by coupling the enhanced moisture conductivity model with chloride transport model.

1. Introduction

Moisture diffusion is a phenomenon that has been studied and explored extensively over the last few decades [1]. Moisture transport in porous media plays an important role in the degradation of construction materials such as mortar and concrete. In particular, the invasion of water in building materials provides a mechanism and path for the penetration of deleterious materials like chloride and sulfate ions. The presence of water can also lead to cracks, which result from freeze/thaw cycles. Clearly an understanding of moisture transport in concrete and mortar is important in order to estimate their service life as construction materials and to improve their quality. The primary transport mechanism of chloride ions ingress into concrete is diffusion and capillary suction. Since diffusion alone can be a very slow process, it may be that capillary transport, especially near the concrete surface is the dominant invasion mechanism. In a reinforced concrete, steel comes under severe corrosion attack by the ingress of chloride ions, which in return causes premature deterioration of concrete. Success of the research on controlling and modeling the ingress of chloride ions is of utmost importance before concrete becomes state-of-the-art construction material for 21st century developments. Against this background, recently several useful methodologies have been proposed in order to assure high durability performance of concrete structures [2–5].

Chloride ingress solely by pure diffusion is a rare occurrence in a marine environment, where civil structures are exposed to continuous wetting and drying by tidal and splash action. When structures are below the low tidal level or constantly submerged, the progress of corrosion will be much limited due to the lack of oxygen supply in underwater environment. Therefore it is very important to consider cyclic wetting and drying conditions in numerical simulation of corrosion progress, which is the root cause of deterioration of concrete structures. In this zone, the rate of chloride penetration is maximized by convection during wetting, and exposure to sufficient atmospheric air brings an inward flow of chloride ions due to high concentration gradient at the surface caused by depleting moisture during drying. However different parts of the same structure are exposed to varied durations of wetting and drying during the same tidal cycle by virtue of their position from the highest tidal level, i.e., the part of the structure close to the high tidal level is exposed to wetting for a very short time during the complete tidal period. On the other hand, the part of the structure which is close to the low tidal level will be exposed to more wetting as compared to drying. Therefore it is very important to simulate the influence of various wetting and drying patterns on the chloride ingress. The objective in this research is to develop a model, which can predict the chloride transport under such turbulent exposures.

In this research real time marine environment phases are modeled in laboratory controlled conditions. And a series of experiments have been performed with different combinations of chloride concentrations (to represent seawater), temperature variations, and wetting/drying spell cycle durations. DuCOM — a durability simulator model of concrete has specifically designed models to tackle with diffusion (vapor transport of moisture) and sorption (liquid transport of moisture) in micro-pore structure of concrete [5]. In this paper the verification and enhancement of liquid transport model of DuCOM has been carried out for its application to marine environment. The

* Corresponding author. Tel.: +81 3 5841 7498; fax: +81 3 5841 6010.
E-mail addresses: princeoneill@hotmail.com (P. O'Neill Iqbal), tetsuya.ishida@civil.t.u-tokyo.ac.jp (T. Ishida).
[1] Tel.: +81 3 5841 7498; fax: +81 3 5841 6010.

0008-8846/$ – see front matter © 2009 Elsevier Ltd. All rights reserved.
doi:10.1016/j.cemconres.2009.01.001

environmental modeling has been carried out by applying hydraulic pressure at the exposed surface elements and numerical analysis is performed by the direct coupling of the enhanced moisture migration model with chloride transport model.

2. Marine exposure environments

The wetting and drying exposure to seawater is the main source of chloride ions ingress and subsequent deterioration of concrete structures along the shorelines. The severe environments of the Middle East, South East Asia and other "hot belt" countries have shown themselves to be particularly harsh on concrete structures subjected to marine conditions. Wetting environments may be classified into humid moist environment, where relative humidity is very near to 100%, and moisture diffuses into the pores by the concentration gradient, and completely submerged environment, where the main transport is due to the capillary suction of liquid water.

3. DuCOM — a thermodynamic durability concrete model

In this research DuCOM model is used, which is the durability computation model developed by Concrete Laboratory–The University of Tokyo, Japan [5]. The originality of this model comes from the fact that DuCOM is a composite multipurpose model, which predicts the state of the concrete from its birth to its entire life. It comprises several sub-models, which work together and are interlinked. The development of multi-scale micro-pore structures at early age is obtained by average degree of cement hydration in the mixture and the amount of hydrated products. For any arbitrary initial and boundary conditions, the vapor pressure in pores, relative humidity (RH), and moisture distribution are mathematically simulated according to a moisture transport model that considers both vapor and liquid phases of mass transport. The moisture distribution, RH, and micro-pore structure characteristics in turn control the Cl^-, CO_2 and O_2 diffusion and rate of carbonation under arbitrary environmental conditions. In this study the chloride transport with moisture migration is the primary focal point. Association map of the whole model is summarized as Fig. 1 [5,6].

4. Governing equation for chloride transport coupled with moisture migration

Chloride transport in cementitious materials under usual conditions is an advective–diffusive phenomenon. In modeling, the advective transport due to bulk movement or pore solution phase is considered, as well as ionic diffusion due to concentration gradients. Mass balance for (moveable) chloride ions can be expressed as shown in Eq. (1) [5].

$$\frac{\partial}{\partial t}(\phi S C_{Cl}) + \mathrm{div} J_{Cl} - Q_{Cl} = 0, \tag{1}$$

Where ϕ: porosity, S: degree of saturation of porous media, and C_{Cl}: concentration of chloride ions in pore solution, and J_{Cl}: total flux of chloride ion. The first term in Eq. (1) represents the rate of change in total amount of chloride ion per unit time and volume, the second term is the flux of chloride ion, and the third term Q_{Cl} is a sink term. Only capillary and gel pores, which can act as transport paths for chloride ions, are considered (the porosity ϕ in Eq. (1) is the sum of the capillary pores and the gel pores).

The flux of chloride ions through a porous body, taking both the diffusion and convection, is expressed by Eq. (2).

$$J_{Cl} = -\frac{\phi S}{\Omega}\delta D_{Cl}\nabla C_{Cl} + \phi S u C_{Cl} \tag{2}$$

where, J_{Cl}: flux of chloride ion (mol/m^2 s), Ω: tortuosity (a reduction factor in terms of complex micro-pore structure), δ: constrictivity (a reduction factor due to the interaction between pore structure and ion transport), D_{Cl}: diffusion coefficient of chloride ion in pore solution (m^2/s), C_{Cl}: concentration of chloride ions in pore solution phase (mol/l), $u^T = [u^x\ u^y\ u^z]$: the velocity vector of ions due to the bulk movement of pore solution phase (m/s), ϕ: porosity of the porous media (m^3/m^3). At the boundary level, the surface flux of chloride ions has been modeled taking into account the diffusion and quasi-adsorption flux (Maruya et al. [7].)

In porous media, the diffusion coefficient is lower than that in the absence of a porous media. Diffusion paths in concrete are constrained because pore structure is tortuous compared with diffusion paths in free liquid and path direction is not parallel to concentration gradient. Tortuosity is introduced to account for this complex micro-pore structure in Eq. (2). This parameter expresses a reduction factor in terms of chloride penetration rate due to complex micro-pore structure. The value of tortuosity changes according to geometric characteristics of the pore structures and it is a function of porosity as [8,9],

$$\Omega = -1.5\tanh\left(8.0\left(\phi_{paste} - 0.25\right)\right) + 2.5 \tag{3}$$

where, $\phi_{paste} = \phi_{cp} + \phi_{gl}$: total paste porosity (m^3/m^3), ϕ_{cp}: capillary zone porosity (m^3/m^3), ϕ_{gl}: gel zone porosity (m^3/m^3), which are

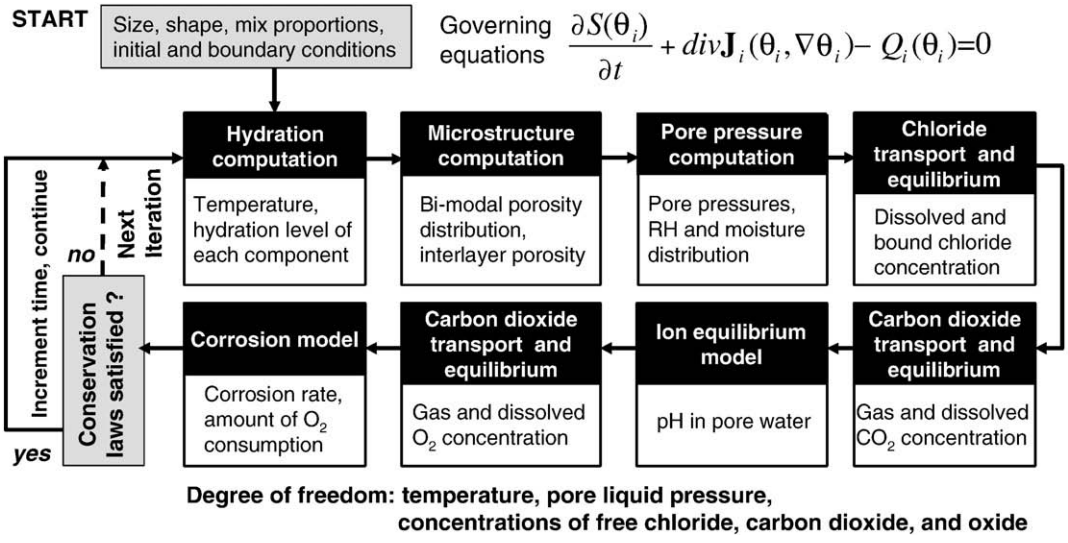

Fig. 1. Basic framework of DuCOM system [5,6].

computed by pore structure development model [5,6]. Another parameter defined as constrictivity considers the effect of interaction between pore structure and ion transport. A constrictivity model for Cl^- (negative ion) in which the effect of ion and pore wall interaction and effect of bound chlorides on the diffusive movement of chloride ions is formulated as,

$$\delta = m \cdot \delta_1 \cdot \delta_2 \tag{4}$$

where, δ_1: reduction parameter for dimensional change and connectivity of the pores, δ_2: reduction parameter for electrical interaction. In the model, it is assumed that δ_1 is a function of computed peak radius of capillary pores, whereas δ_2 is a function of the amount of bound chloride. Here, a new hypothesis was made that when bound chlorides increase, the diffusion rate of chloride ions moving through the pore water is reduced by the increase in the adsorbed component (adsorbed chlorides) on the pore. It is assumed that as the adsorbed chlorides on pore wall increase, the chloride ions passing through the narrow pore spaces are acted upon electrically by the negatively charged adsorbed chlorides, and as a result the diffusion rate would be reduced. Further detailed descriptions can be found in the literature [9].

The relationship between chloride ions and bound chlorides under equilibrium condition is modeled as Langmuir type equation based on experiments [10] as,

$$C_b = \frac{\alpha \cdot C_f}{1 + 4.0 C_f} \tag{5}$$

where, C_b: concentration of bound chlorides (% by mass of binder), C_f: concentration of chloride ions (% by mass of binder). The binding capacity varies depending on the cement mineral composition, the types of admixtures, and the replacement ratio, etc. These effects are expressed by a parameter α in Eq. (5). Based on experimental data [10] α is formulated for ordinary Portland cement (OPC), blast furnace slag (BFS) and fly ash (FA).

$$\begin{array}{ll} a = 11.8 & \text{OPC} \\ a = -34.0 \cdot b^2 + 13.3 \cdot b + 11.8 (0 \le b \le 0.6) & \text{BFS} \\ a = -15.5 \cdot f^2 + 1.8 \cdot f + 11.8 (0 \le f \le 0.4) & \text{FA} \end{array} \tag{6}$$

where, b and f, are the replacement ratios by mass of blast furnace slag and fly ash, respectively.

The second term in Eq. (2) represents the convection transport of chloride ions due to bulk movement of liquid water in the porous media. It is here the chloride transport model and moisture migration model are coupled to simulate the interlinked phenomenon of chloride advection with moisture currents. Therefore the moisture movement into and out of the system directly affects the chloride distribution in the same way as is happening in the real diffusion–convection marine environment. This issue will be discussed in the following chapters.

5. Modeling of liquid conductivity in DuCOM

Moisture migration is the combination of potential gradients of temperature, vapor pressure, with liquid conductivity. In DuCOM all these mechanisms are modeled considering their physical behavior [5,11]. The moisture transport model for cementitious materials considers the multiphase dynamics of liquid and gas phases. The contributions of the diffusive as well as bulk movements of moisture have been combined in the model. The total porosity of the cementitious material is divided into interlayer, gel and capillary porosity. The moisture model considers the contributions from each of these components from a thermodynamic viewpoint. The macroscopic moisture transport characteristics of flow, such as conductivity are obtained directly from the microstructure of the porous media, and this is achieved by considering the mass conservation of moisture capacity, conductivity, pore-structure development, and moisture loss due to hydration.

The moisture capacity is obtained from pore structures, summation of gel, capillary and interlayer. Moisture conductivity comprises of liquid and vapor phases computed from pore structure. Pore structure development is based on cement particle expansion, and average degree of hydration, and lastly moisture loss due to hydration is directly obtained from hydration model in DuCOM [5].

The total moisture flux J [kg/m^2 s] for both vapor and liquid can generally be expressed as [5,6,11]

$$J = (q_v + q_l) \tag{7}$$

Where q_v is the vapor flux and q_l is the liquid flux in kg/m^2 s. The flux of liquid water q_l [kg/m^2 s] can be calculated using the following model based on Darcy's Law.

$$q_l = -\frac{\rho_l \phi^2}{50\eta}\left(\int_0^{rc} r dv\right)^2 \nabla P_l = -K_l \nabla P_l \tag{8}$$

Where, K_l: liquid conductivity [kg/Pa m s]. ρ: density of liquid water kg/m^3, ϕ: porosity of concrete m^3/m^3. From the viewpoint of temperature changes, the most significant factor affecting liquid water transport is the viscosity η [Pa s] of liquid water. Actually the water present in the cementitious microstructure is far from the ideal condition. Such a non-ideal behavior may result from the dissolution of salts, the long-range forces exerted on the water molecules from the surrounding porous medium, the effects of the polarity of water, or a complex combination of any of these factors [6]. From a thermodynamic point of view the actual viscosity of the fluid under non-ideal conditions at an absolute temperature T is given by Eq. (9) [6].

$$\eta = \eta_i \exp\left(\frac{G_e}{RT}\right) \tag{9}$$

Where, η_i: viscosity of liquid water under ideal conditions, R: universal gas constant, T: temperature and G_e: additional Gibbs energy required for liquid flow under non-ideal conditions.

The actual permeability of water can be evaluated if the effect of the non-ideal viscosity of water is taken into account. Past researchers have reported a viscosity that is about one or two orders higher than the ideal viscosity of water when measured under thin quartz plates [12]. When concrete is exposed to water, a transient phase of apparent reduction in the water permeability is observed until it reaches a final value, which is smaller than the permeability expected under ideal conditions. To simulate such a time dependent behavior, a hypothesis was made that there exist a pore-water and microstructure interaction which is a time lag phenomenon, bringing about the change in the state of pore water from ideal to non-ideal state and roughly depends on the history of pore humidity.

The physical significance of this model is to simulate the reaction of two different micro-pore structures (fine and coarse micro-pore) towards the same external humidity. Clearly a fine or dense micro-pore concrete will react to the change in external humidity much slower as compared to the concrete with a coarse micro-pores. In this computational model, a simple Kelvin Chain model represents this phenomenon, where the dashpot viscosity η_d represents the responsiveness of the microstructure to changes in the actual pore humidity, H that brings about a change in pore wall humidity also called as dash-pot humidity H_d. The goal through this model is to obtain the extra energy, G_e required for the activation of flow at any point and time, such that the effective non-ideal viscosity of the pore fluid, η, and the effective permeability can be computed [6].

Table 1
Specimen identification table.

Shape	Temperature °C	w/c %	Cement kg/m^3	Sand kg/m^3	Water kg/m^3
Cylinder	20	50	580	1305	290
		35	635	1429	222
Cylinder	40	50	580	1305	290
		35	635	1429	222

The computational model is given by

$$G_e = G_{max} H_d \tag{10}$$

$$H'' d + \left(\frac{1+\eta_d''}{\eta_d}\right) H_d = \frac{H}{\eta_d} \tag{11}$$

$$\eta_d = a(1 + bH_d^c) \tag{12}$$

$$a = \left[1.59\left(\frac{\phi - \phi_m}{\phi_m}\right) + 0.70\right]^5 \tag{13}$$

$$b = 2.5a \quad \text{and} \quad c = 2.0$$

Where G_{max} is the maximum additional Gibbs energy for the activation of flow = 3000 kcal/mol, ϕ is the total suction porosity, and ϕ_m is the viscosity accessible by mercury intrusion (Gel and capillary zone porosity).

6. Proposed modeling of submerged environment in DuCOM

Since convection (transport of chloride ions with moisture flow in concrete) is one of the major causes of chloride transport in wetting and drying environments, hence in this section, the emphasis is laid on the transport of moisture from the exposed surface towards inner core. For moisture movement dominant in vapour form, the surface mass flux is given by the following Eq. (14) as,

$$q_s = -E_b(h - h_s) \tag{14}$$

Where, E_b is the emissivity coefficient and a value of 5×10^{-5} is given to the constant. h is the relative humidity of the interior and h_s is the relative humidity of the surrounding environment. This equation is valid for the case where moisture transport takes place mainly in vapor form, such as exposure to drying or moisture adsorption [13].

In the above equation, the environmental relative humidity h_s as well as that of the interior can be correlated to the pore pressure head. The relationship between the pore pressure P_l and the relative humidity h is described by the following Kelvin's equation.

$$P_l = \frac{\rho RT}{M} \ln h \tag{15}$$

Where, ρ is the density of liquid water, M is the molecular mass of liquid, R is the universal gas constant, and T is the absolute temperature. Relative humidity in Eq. (15) h has a domain from 0 to 1.0, i.e., the surrounding humidity value ranges from 0% (completely dry air) to 100% (fully saturated air). As found in the formulation, from a theoretical viewpoint, both these extremes are singularity points for Kelvin's equation. Another important aspect of this equation is that it always gives negative value of pore pressure for any value of relative humidity.

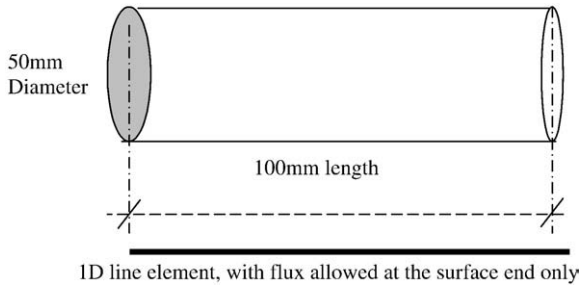

Fig. 2. FEM 1-D element for cylindrical specimen.

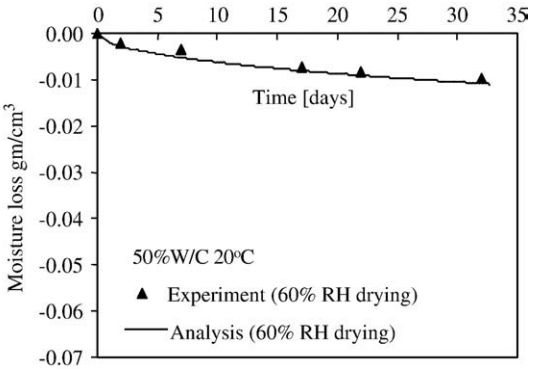

Fig. 3. Experiment and analysis for drying at 60% RH environment for 50%w/c.

In water submerged environment, however, hydraulic pressure acts on the exposed surface, and moisture moves under the positive pore pressure head. This condition cannot be reproduced by Kelvin's equation, even though a value sufficiently close to 100% is given. In other words, the completely saturated conditions can never be simulated, which always ends up in suction pressure (negative pore pressure).

To distinguish the water submerged conditions from un-saturated humid environment, there are two options to define the boundary conditions in the analytical system. For water submergence, positive pressure equal to the hydraulic head of water is applied to the exposed surface, whereas for un-saturated environment, the negative pore pressure computed by Kelvin's equation Eq. (15) is used. In the following verifications, submerged environments (completely saturated condition) is reproduced by applying hydraulic pressure at the surface node of the elements so that the sorption flux of liquid water can be simulated by more realistic manner, and the influence of different boundary conditions (such as the difference between complete submerged conditions and high humid conditions) on coupled moisture and chloride transport will be studied.

Application of hydraulic pressure at the surface nodes of elements is desirable for situations where there is water submergence after long period of drying, or for alternate wetting and drying environments.

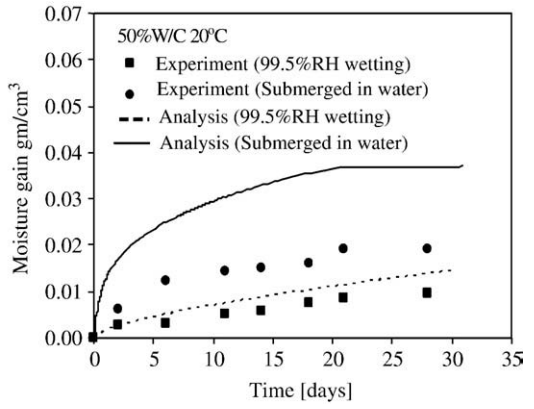

Fig. 4. Experiment and analysis for wetting at 99.5% RH and submerged environment for 50%w/c.

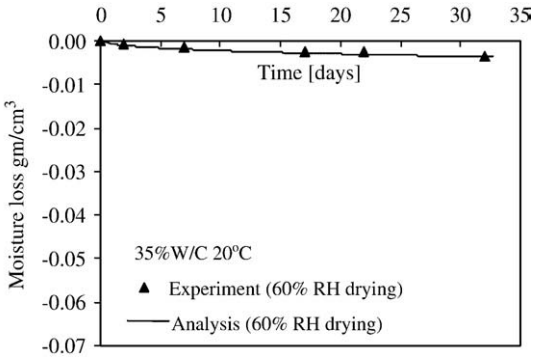

Fig. 5. Experiment and analysis for drying at 60% RH environment for 35%w/c.

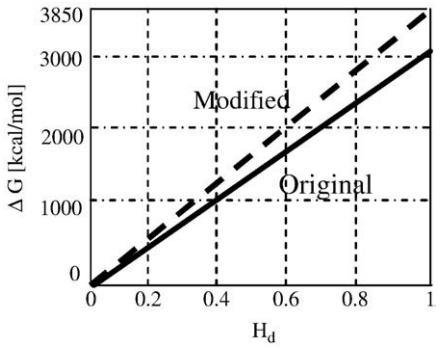

Fig. 7. Relation between Gibbs factor and fictitious humidity.

Hence DuCOM has the capability to represents both the unsaturated environment as well as completely saturated conditions.

7. Experimental verification of moisture conductivity model

Cylindrical specimens of 50 mm diameter and 100 mm height were prepared. After casting, all the specimens were sealed and cured for 28days at 20 °C. Then the cylindrical specimens were coated with epoxy to make them water tight and a 4 mm slice was cut from the top surface with a concrete cutter. All the specimens were placed inside an environment control chamber at 60% relative humidity (RH) with 20 °C and 40 °C temperatures for 30 days. After this exposure, the respective specimens were exposed to a 99.5% relative humidity environment and water submerged conditions for another 30 days. During drying at 60% RH, wetting at 99.5% RH and water submergence, the weight loss/gain readings were taken regularly by an electronic weighing machine sensitive to two decimal places.

7.1. Material and specimen preparation

Ordinary Portland cement, regular tap water, coarse sand and a W/C of 50% and 35% were provided to all specimens. The mix proportion of cement-to-sand was kept at 1:2.25. Cement, sand and water contents are provided as shown in Table 1.

7.2. Analytical boundary conditions

The boundary conditions in the modeling are simulated as outlined for the experiment. For the initial curing period, moisture flux in and out of the specimen is restricted, whereas heat flux is allowed during curing and environment exposure conditions. The humid wetting cycle is modeled by providing 99.5% RH (since the environmental chamber is capable of producing 99.5% RH) and drying environment corresponds to 60% RH. To simulate the water-submerged case, hydraulic pressure is applied to the surface (boundary) elements. The cylindrical specimen with only top surface exposed to the environment is modeled by considering a line elements with flux allowed at the surface element only as shown in Fig. 2.

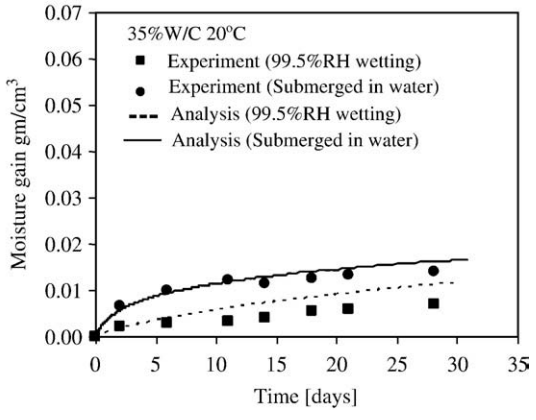

Fig. 6. Experiment and analysis for wetting at 99.5% RH and submerged environment for 35%w/c.

7.3. Experiment results and discussion

Figs. 3 and 4 correspond to coarse micro-pore structure (50%w/c) for drying at 60% relative humidity and wetting at 99.5% relative humidity as well as water submerged condition. On the other hand, Figs. 5 and 6 correspond to dense micro-pore structure (35%w/c). From these results, it may be seen that the moisture migration model for vapor conductivity is very good, which can nicely predict the flow dominated by vapor flux at 60% and 99.5% relative humidity for 50% and 35% w/c cases. However, the liquid flow in case of coarse micro-pore structure (50%w/c) is overestimated.

8. Enhancement in liquid conductivity model

By the experiment results shown in Section 7.3, it was observed that the moisture conductivity model overestimates for coarse micro-pore structure (high water-to-cement ratio). Hence the need arises to enhance the parameters of liquid flux equation (Eq. (8)). In this equation, the density is constant for liquid water at a given temperature. The porosity of concrete comes from micro-pore structure model, which is already well integrated and verified by past research [5,6]. However the non-ideal viscosity has a room for improvement because of insufficient experimental verification, especially for coarse micro-pore structure.

Therefore enhancement was proposed, in such a way that the non-ideal viscosity of liquid water in coarse micro-pore structure is

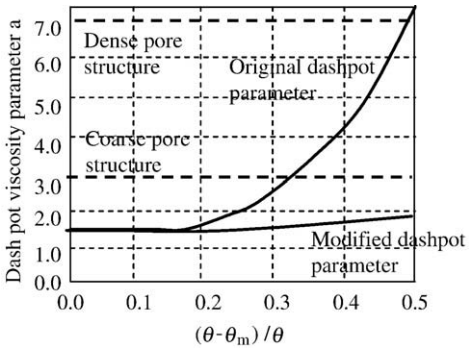

Fig. 8. Relation between dashpot viscosity parameter and porosity.

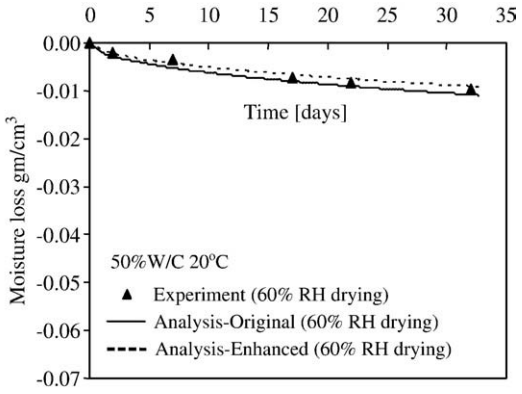

Fig. 9. Experiment and analysis for drying at 60% RH environment for 50%w/c at 20 °C.

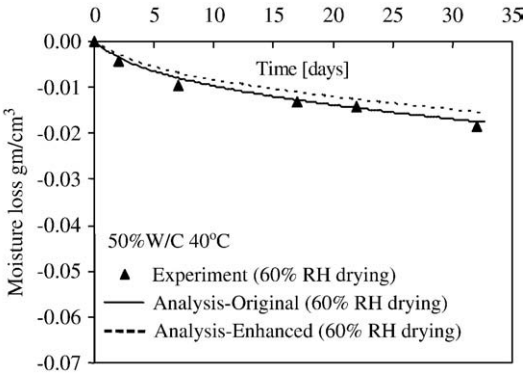

Fig. 11. Experiment and analysis for drying at 60% RH environment 50%w/c at 40 °C.

increased, whereas for dense micro-pore structure it remained same by the combination of Gibbs factor and dashpot viscosity parameter. In the enhanced model G_{max} was increased from 3000 kcal/mol to 3850 kcal/mol. However by increasing only the maximum Gibbs energy, the analysis for dense micro-pore structure will give under-estimation. Therefore to make the liquid conductivity model equally applicable to any kind of micro-pore structure, the sensitivity of dense micro-pore concrete was decreased by softening the dash-pot viscosity parameter 'a' with minimum affect on coarse micro-pore concrete as shown in Fig. 8. The enhanced equation for dash-pot viscosity parameter is given as Eq. (12). Therefore the combined affect of this enhancement is to increase the viscosity of liquid flow in dense micro-pore structure only. In this way the model can be universally applicable to dense and coarse micro-pore structures. Fig. 7 shows the relationship between original and enhanced Gibbs energy and fictitious humidity H_d.

$$a = \left[1.59\left(\frac{\phi - \phi_m}{\phi_m}\right) + 0.85\right] \tag{16}$$

9. Analysis with enhanced liquid conductivity model

Figs. 9–12 correspond to the moisture gain and loss for 50% water cement ratio concrete at 20 °C and 40 °C temperatures, whereas Figs. 13–16 correspond to 35% water cement ratio. In these results comparisons is made between experiment and analysis for drying at 60% humidity, wetting at 99.5% humidity and water submerged environment. The analysis by using enhanced liquid conductivity model shows very good results for both high and low water cement

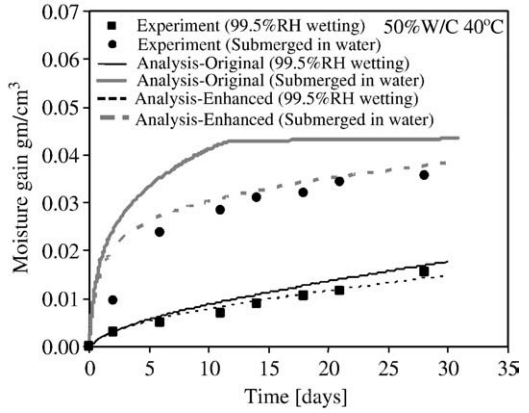

Fig. 12. Experiment and analysis for wetting at 99.5% RH and submerged environment 50%w/c at 40 °C.

ratio concretes at 20 °C and 40 °C temperatures. The viscosity reduction for high w/c concrete by the combined affect of Gibbs factor and Dashpot viscosity parameter nicely simulate the experimental results. Also the already correct results for low w/c are preserved with the less sensitive dashpot viscosity parameter in combination with increased Gibbs Factor. A slight reduction in moisture gain and loss is seen for the case of relative humid environments, due to the increased viscosity of flow. But since the main transport of moisture under humid environments is in vapor form, therefore these results are not so much affected by this enhancement. It has to be noted that the

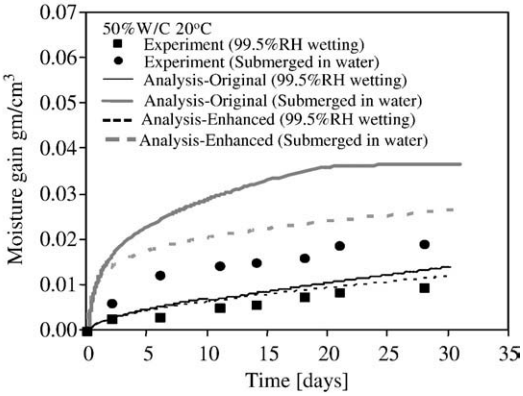

Fig. 10. Experiment and analysis for wetting at 99.5% RH and submerged environment for 50%w/c at 20 °C.

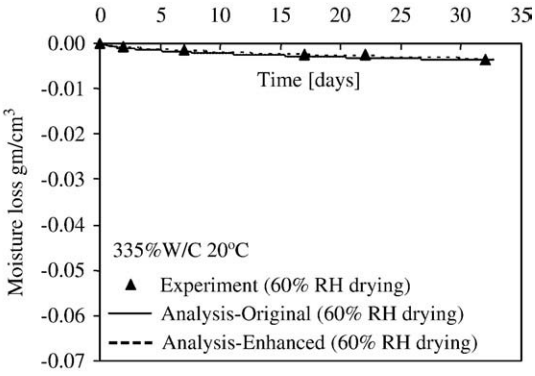

Fig. 13. Experiment and analysis for drying at 60% RH environment 35%w/c at 20 °C.

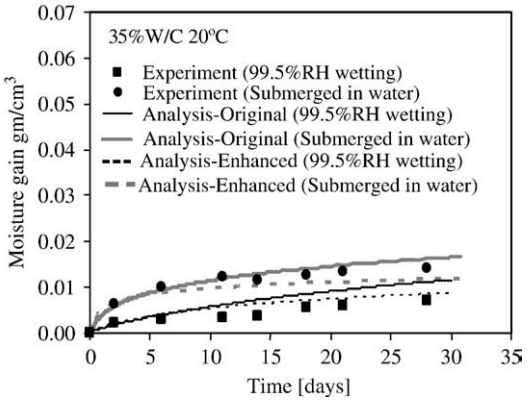

Fig. 14. Experiment and analysis for wetting at 99.5% RH and submerged environment 35%w/c at 20 °C.

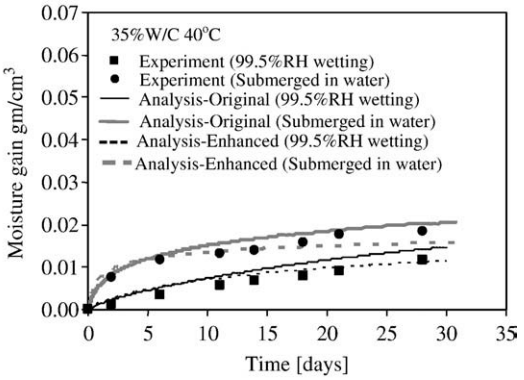

Fig. 16. Experiment and analysis for wetting at 99.5% RH and submerged environment 35%w/c at 40 °C.

original moisture migration model predicts very nicely for unsaturated conditions, as shown by these results.

10. Chloride transport under alternate wetting and drying (marine) environments

Alternate wetting and drying is a typical marine environment. To model moisture migration in marine environment, this hygral wetting and drying must be considered.

Fig. 17 shows wetting and drying effects on a concrete wall due tidal rise and fall. The wetting very near to the high tidal level is very less, which increases linearly as the low tidal level is approached. Considering this pattern, three alternate wetting and drying cycles are designed in laboratory-controlled environment as 1% wet–99%dry, 10% wet–90% dry and 40% wet–60% dry cases. These exposure cycles are shown in Fig. 18.

10.1. Material and specimen preparation

Ordinary Portland cement, regular tap water, coarse sand and a w/c of 50% was provided to all specimens. The mix proportion of cement to sand was kept at 1:2.25. Cement content 580 kg/m^3, water 290 kg/m^3 and sand 1305 kg/m^3 were used. Specimens consist of cylinders 50 mm diameter and 100 mm height. Curing was done for 28 days in sealed condition at 20 °C temperature. After curing, the top 4 mm slice from the surface of all the specimens was removed to minimize the surface disturbances. Dry cutting was done for slicing of the specimens.

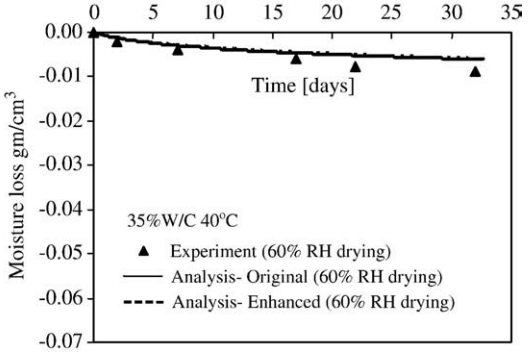

Fig. 15. Experiment and analysis for drying at 60% RH environment 35%w/c at 40 °C.

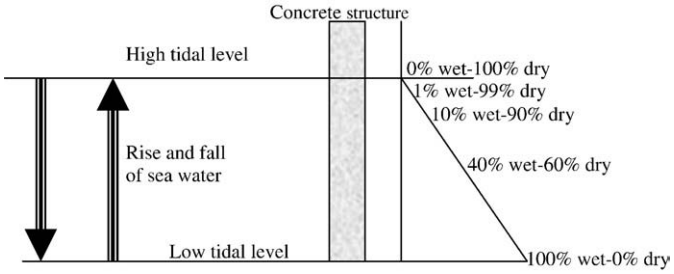

Fig. 17. Wetting and drying in marine environment.

10.2. Specimen preparation for chloride testing

For the determination of chloride profiles, specimens were tested after 1, 7 and 12 months exposure by potentiometer titration technique. In this experiment, slicing method was used for the determination of chloride contents. Thickness of each slice was measured and specimen loss due to the blade thickness of the cutter

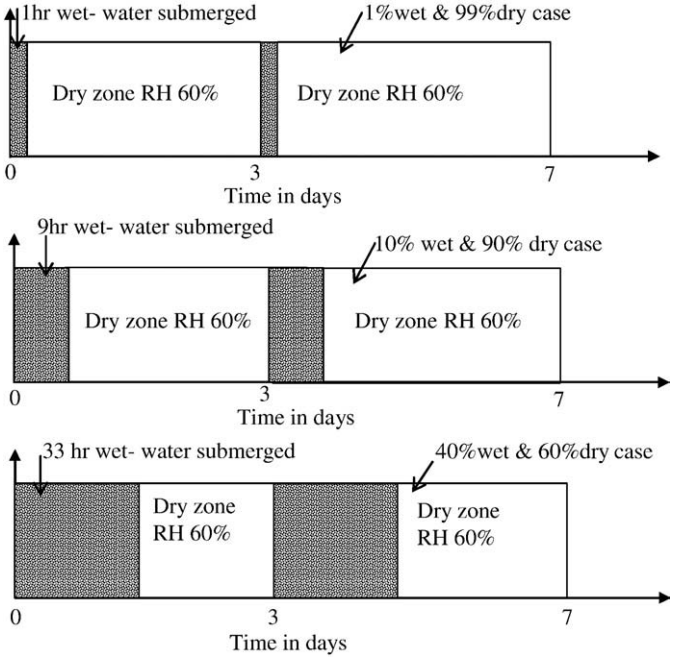

Fig. 18. Weekly exposure cycle for alternate wetting and drying experiment.

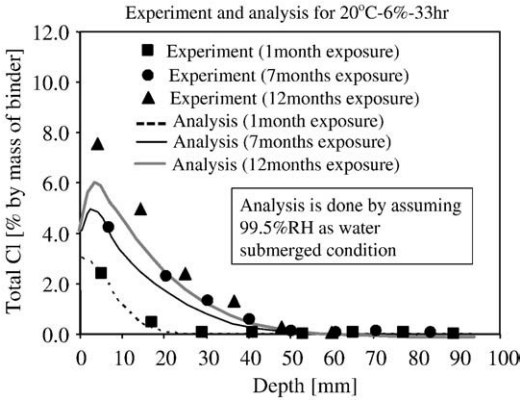

Fig. 19. Experiment and analysis comparison for 1, 7 and 12 months for 33 h wetting.

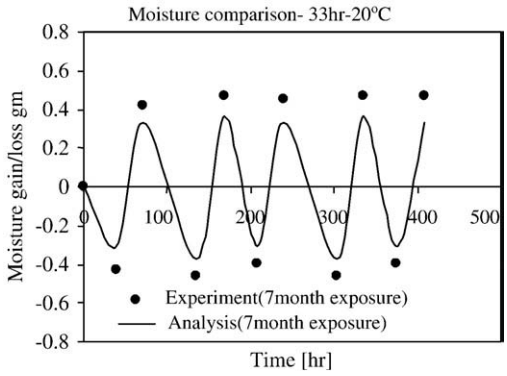

Fig. 21. Moisture migration results by assuming 99.5% RH as submergence for 33 h wetting.

was accounted for in measuring the depth of each slice from the surface. After this, the slices of respective specimens were grounded and tested for the chloride contents according to the relevant ASTM standard C1152/C1152M-04 (for acid soluble chloride) [13].

10.3. Analytical boundary conditions

The boundary conditions in the modeling were simulated as precise as in the experiment. In the modeling, only one surface was exposed to the environment to simulate the sealed specimen with one face exposed. For the initial curing period, the moisture flux in and out of the specimen was restricted, whereas the heat flux was allowed during curing and environment exposure conditions. The submerged wetting cycle was modeled by applying hydraulic head of water as well as by providing 99.5% relative humidity and drying environment corresponds to 60% RH.

During the experiment, a water layer was observed on the surface of the vertically placed specimens during drying. For all the specimens, the wet surface remained for 4 h. Thus, this condition is modeled in the analysis by increasing the wetting duration by 4 h, and subsequently decreasing the drying time by 4 h. The relative humidity at the surface becomes equal to the surrounding environment (60%) as it reaches to air dry state. This condition remains stable throughout the drying period, and is simply modeled with 60% RH with moisture flux allowed at the surface.

10.4. Analysis by considering 99.5% RH as water submerged condition

Firstly, analysis is carried out by modeling the moisture migration by using Kelvin equation (Eq. (15)). In this analysis, a value of 99.5% relative humidity was given as a boundary condition, since Kelvin equation cannot deal with completely saturated conditions, namely 100% RH, which corresponds to the singularity point as already discussed in earlier sections.

Figs. 19 and 20 show the experimental and analytical chloride penetration profiles for 33 h wetting case for 3% and 6% NaCl by mass of water respectively at 20 °C. Fig. 21 is the corresponding moisture gain and loss for 33 h wetting case. It can be seen that slight under-estimation is seen in the analytical chloride profiles. The same trend of under-estimation is observed in the corresponding moisture migration analysis in Fig. 21. The under-estimation is due to the assumption

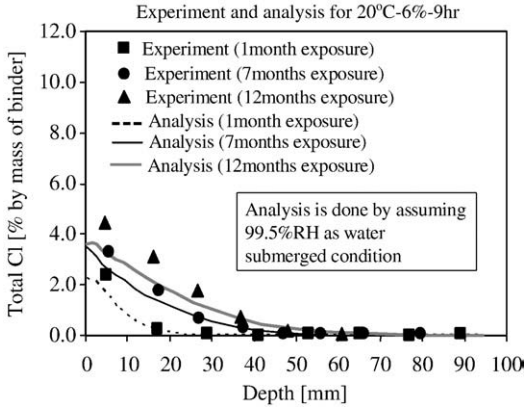

Fig. 22. Experiment and analysis comparison for 1, 7 and 12 months for 9 h wetting.

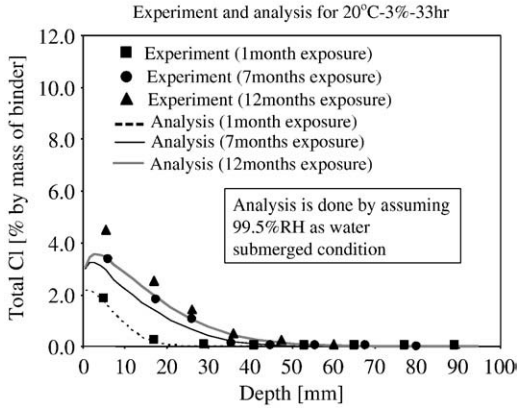

Fig. 20. Experiment and analysis comparison for 1, 7 and 12 months for 33 h wetting.

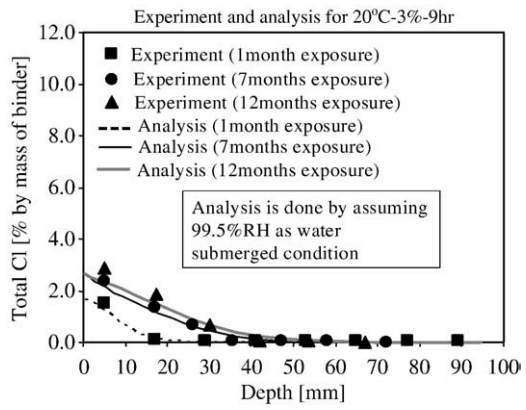

Fig. 23. Experiment and analysis comparison for 1, 7 and 12 months for 9 h wetting.

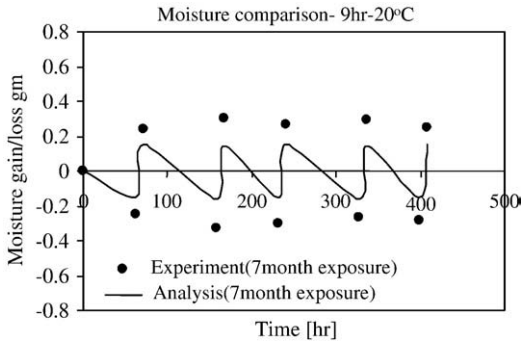

Fig. 24. Moisture migration results by assuming 99.5% RH as submergence for 9 h wetting.

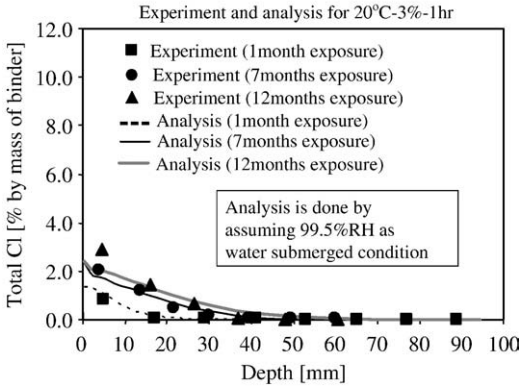

Fig. 26. Experiment and analysis comparison for 1, 7 and 12 months for 1 h wetting.

of 99.5% relative humidity as water submerged conditions. In reality it is not possible to know the affect of 99.5% relative humidity exposure on chloride transport, but in analysis it can be simulated and logical under-estimation is observed.

Figs. 22 and 23 are the experimental and analytical chloride penetration profiles for 9 h wetting case for 3% and 6% NaCl by mass of water respectively at 20 °C. Fig. 24 is the corresponding moisture gain and loss for 9 h wetting case. Similarly Figs. 25 and 26 are the experiment and analytical chloride penetration profiles for 1 h wetting case for 3% and 6% NaCl by mass of water respectively at 20 °C. Fig. 27 is the corresponding moisture gain and loss for 1 h wetting case.

In all the wetting and drying cases under-estimation is seen in the analytical chloride profiles. The same trend of under-estimation is observed in the corresponding moisture migration results, which shows the strong coupling between moisture migration and chloride transport. This underestimation is due to the use of simplified method of assuming 99.5% RH as water submergence. In this section liquid transport is modeled with 99.5% relative humidity (un-saturated condition), and therefore under-estimation is observed in the analysis. A more refined and precise way of treating this alternate wetting and drying environment is by applying hydraulic pressure at the surface elements.

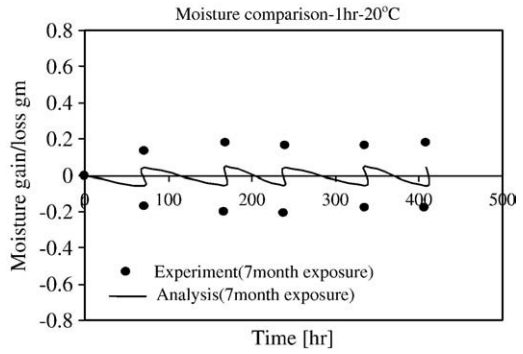

Fig. 27. Moisture migration results by assuming 99.5% RH as submergence for 1 h wetting.

10.5. Analysis by hydraulic pressure (saturated pore pressure)

The method of application of hydraulic pressure (saturated pore pressure) is applied to model alternate wetting and drying for 33 h, 9 h and 1 h wetting cycles. The experimental and analysis result shown in Fig. 28–33 corresponds to 33 h, 9 h and 1 h wetting cycles for 6%NaCl at 20 °C. In this section, analysis is done by the application of hydraulic pressure, which corresponds to completely saturated environment. It may be seen that the underestimation by assuming 99.5% RH as water submergence is eliminated in this method. The moisture migration analysis also matches up nicely with the experimental data. For the highly eccentric case of 1 h wetting (Fig. 32), there is slight over-estimation in the analysis for chloride transport. The same trend can be seen in the corresponding moisture migration analysis in Fig. 33. Although the model still needs more enhancements for such an extreme cases, overall behaviors are well simulated.

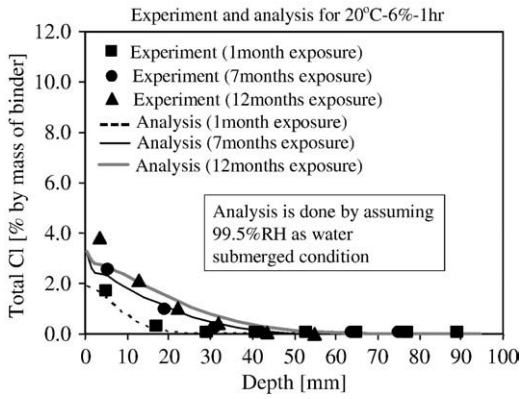

Fig. 25. Experiment and analysis comparison for 1, 7 and 12 months for 1 h wetting.

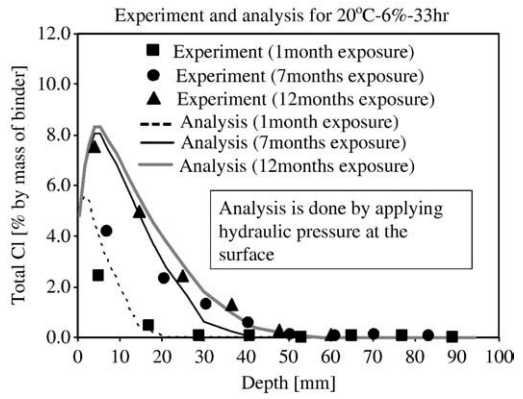

Fig. 28. Chloride penetration profiles by hydraulic pressure for 33 h wetting.

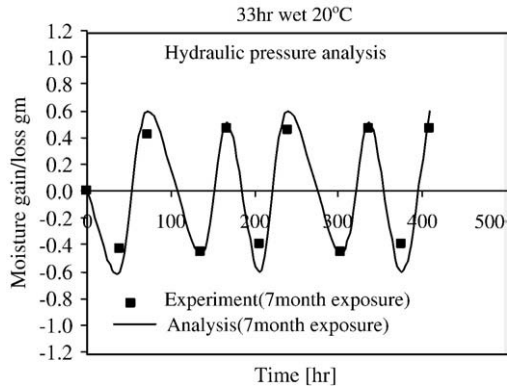

Fig. 29. Moisture migration by hydraulic pressure for 33 h wetting.

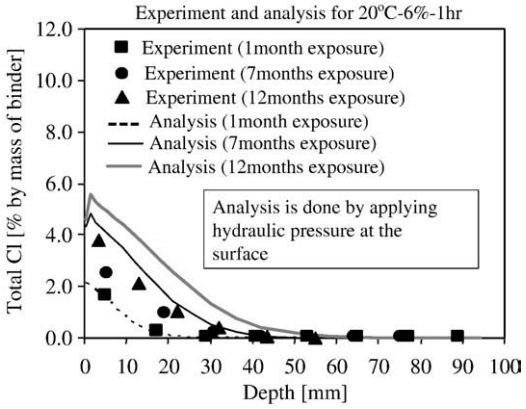

Fig. 32. Chloride penetration profiles by hydraulic pressure for 1 h wetting.

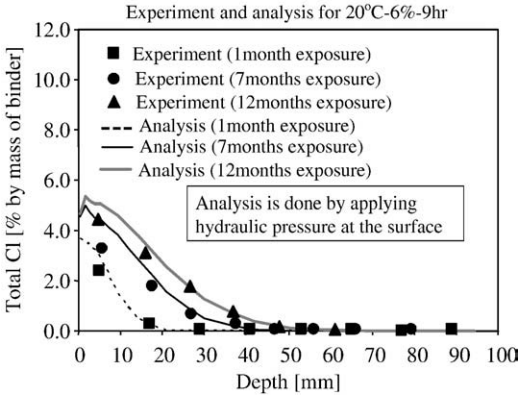

Fig. 30. Chloride penetration profiles by hydraulic pressure for 9 h wetting.

10.6. Strong coupling between chloride and moisture model

The analysis results for chloride transport and corresponding moisture migration show strong coupling in the experimental as well as analytical results. An increase in moisture gain and loss significantly amplify the chloride penetration depths and concentration. This is due to the strong convection flux of chloride ions generated by wetting and drying cycles. The physical phenomenon of convection transport of chloride ions is simulated by coupled modeling of chloride transport and moisture migration results. This strong coupling between chloride and moisture migration also clearly showed the affect of liquid transport on chloride ingress. Clearly chloride penetration is much affected if unsaturated conditions of 99.5% relative humidity are given as boundary conditions in the Kelvin equation. However, if completely saturated environment is modeled by applying hydraulic pressure (saturated pore pressure), chloride penetration matches up nicely with the experiment.

11. Conclusions

In this research, a unique approach is adopted to simulate saturated conditions in a typical marine environment for alternate wetting and drying as well as single long wetting exposure. DuCOM carries out both un-saturated and completely saturated wetting environment modeling. The liquid conductivity model is enhanced for sorption absorption. To model continuous alternate wetting and drying marine environments, analysis was made by assuming 99.5% relative humid environment (near to saturated conditions), which shows underestimation in the chloride penetration along with the moisture loss and gain results. However if completely saturated conditions are modeled by taking positive pore pressure as a degree of freedom, the analysis for chloride transport shows good results. The application of hydraulic pressure is effective to determine strong sorption flux, which is triggered after prolonged drying and for environments alternate with wetting and drying. This kind of analytical approach is highly advantageous for tidal and splash zones.

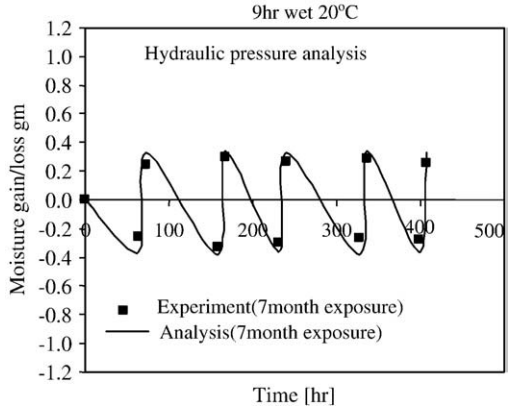

Fig. 31. Moisture migration by hydraulic pressure for 9 h wetting.

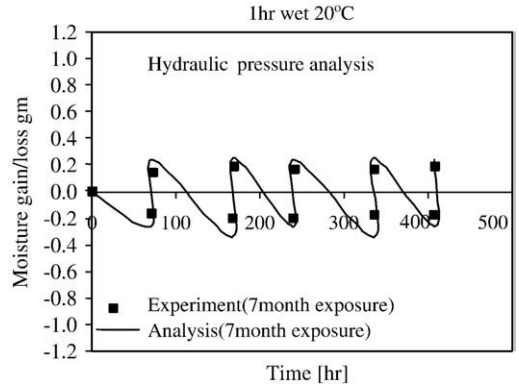

Fig. 33. Moisture migration by hydraulic pressure for 1 h wetting.

References

[1] Z.P. Bazant, L.J. Najjar, Nonlinear water diffusion in nonsaturated concrete, Materials and Structures 5 (1) (1972) 3–20.
[2] E. Samson, J. Marchand, K.A. Snyder, J.J. Beaudoin, Modeling ion and fluid transport in unsaturated cement systems in isothermal conditions, Cement and Concrete Research 35 (2005) 141–153.
[3] L. Nilsson, T. Luping, Interaction and its effect on substance transport in concrete, Proceedings of the international conference on Ion and Mass Transport in Cement Based Materials, 1999, pp. 155–180, Toronto, Canada.
[4] V. Baroghel-Bouny, Durability indicatiors: relevant tools for performance-based evaluation and multi-level prediction of RC durability, Proceedings of the International RILEM workshop on Performance based evaluation and indicators for concrete durability, 2006, pp. 3–29, Madrid, Spain.
[5] K. Maekawa, T. Ishida, T. Kishi, Multi-scale modeling of concrete performance—integrated materials and structural mechanics, Journal of Advanced Concrete Technology, JCI 1 (2) (July 2003) 91–126.
[6] K. Maekawa, R. Chaube, T. Kishi, Modelling of Concrete Performance, E&FN SPON, 1999.
[7] T. Maruya, Y. Matsuoka, S. Tangtermsirikul, Simulation of chloride movement in hardened concrete, Concrete Library of JSCE 20 (1992) 57–70.
[8] K. Nakarai, T. Ishida, K. Maekawa, Multi-scale physicochemical modeling of soil—cementitious material interaction, Soils and Foundations 46 (5) (October 2006) 653–664.
[9] T. Ishida, P. Iqbal, and T.L.A. Ho, Modeling of Chloride Diffusivity Coupled with Non-linear Binding Capacity in Sound and Cracked Concrete, Cement and Concrete Research (under review).
[10] T. Ishida, S. Miyahara, T. Maruya, Chloride binding capacity of mortars made with various Portland cements and mineral admixtures, Journal of Advanced Concrete Technology 6 (2) (2008) 287–301.
[11] T. Ishida, K. Maekawa, T. Kishi, Enhanced modeling of moisture equilibrium and transport in cementitious materials under arbitrary temperature and relative humidity history, Cement and Concrete Research 37 (2007) 565–578.
[12] G. Peschel, The viscosity of thin water films between two quartz plates, Matrix et Construction 1 (N6) (1968) 529–534.
[13] ASTM standard designation C1152/C1152M-04 Standard Test Method for Acid Soluble Chloride in Motor and Concrete.